Exciton Recombination Radiation and Phonon Spectrum of 6*H* SiC

W. J. Choyke and Lyle Patrick
Westinghouse Research Laboratories, Pittsburgh, Pennsylvania
(Received May 10, 1962)

A photoluminescence spectrum consisting of about 50 lines has been observed at low temperatures in 6*H* SiC. The spectrum can be attributed to exciton recombination after capture by un-ionized nitrogen atoms. The mechanism is similar to that first reported by Haynes for impurities in Si, but the large unit cell of 6*H* SiC (with 12 atoms) provides three inequivalent sites for nitrogen, and 36 phonon branches, hence the large number of lines. Seventeen phonon energies have been measured and plotted in a plausible way in an appropriate extended **k** space, leading to some conclusions about the band structure of 6*H* SiC. Spin-orbit splitting of the valence bands is only 4.8 meV suggesting that the hole is confined to the carbon sublattice. Luminescence, due to the annihilation of free excitons, has also been observed. Earlier absorption measurements have been reinterpreted, making use of the new understanding of the 6*H* SiC phonon spectrum.

I. INTRODUCTION

RECENT measurements[1–3] have shown the importance of excitons in the low-temperature absorption and photoluminescence spectra of Ge and Si. Excitons are perhaps even more important in 6*H* SiC because of the greater exciton binding energy, due to the greater carrier masses in 6*H* SiC. The absorption edge of 6*H* SiC, like those of Ge and Si, is due to indirect transitions which produce excitons.[4] The annihilation, or recombination of these excitons, excited by uv illumination at low temperatures, gives rise to the spectra reported here. We have not observed any luminescence attributable to the recombination of free electrons and holes. 6*H* SiC differs from Ge and Si in having a partly ionic lattice,[5] a large energy gap ($\sim$3 eV), a uniaxial crystal structure ($P6_3mc$) and, most important for the present experiment, a crystal structure with a large unit cell.

We shall describe two spectra, one due to recombination of free excitons (the *intrinsic* spectrum), and the other due to recombination of excitons bound to un-ionized nitrogen atoms (the *nitrogen* spectrum). Nitrogen substitutes for carbon in SiC and is a donor.[6] When the un-ionized donor captures an exciton, a four-particle complex is formed, consisting of the donor ion and three electronic particles.[7] Electron-hole recombination within a four-particle complex is what we mean by exciton recombination at an impurity atom.

Recombination within such a complex was first reported by Haynes[2] for Si, and has probably been observed in Ge also.[3] The impurity exciton spectrum in Si is displaced in energy by the amount of the binding energy of the exciton to the impurity, and an additional line appears, due to the possibility of recombination *without* phonon emission, since the exciton is localized.

In 6*H* SiC the impurity spectrum, in our case the *nitrogen* spectrum, differs from that in Si in its complexity, having about 50 resolvable lines, all of which can be shown to arise from exciton recombination at nitrogen atoms only. There are two reasons for the great number of lines, both attributable to the large unit cell. (1) In 6*H* SiC there are three inequivalent carbon sites,[8] hence, three different kinds of nitrogen donors, resulting in three distinct series of lines. (2) Each series of lines is unusually complex, because the 12 atoms per unit cell result in 36 branches in the phonon spectrum; it is more convenient, however, to think of 6 branches in a momentum space extended 6 times along the hexagonal axis, with the possibility of energy discontinuities and umklapp processes within the extended zone. The intrinsic spectrum, due to recombination of free excitons, is complicated only by the second of the above two factors.

The experimental results fall naturally into four parts, so we shall present them in four sections (IV to VII), including in each section an interpretation of that portion of the data. Brief summaries of these four sections follow.

In Sec. IV we show the nitrogen spectrum at 6°K and indicate how we can identify the lines in one of the three series of lines. The only complexity then remaining in this series of lines is that of the phonon spectrum. We measure 17 phonon energies and plot them in a plausible way in an extended **k** space to obtain a much more detailed phonon spectrum than one finds by similar measurements in semiconductors with simple unit cells. We draw certain conclusions about the positions of the conduction-band minima. The energies by which the excitons are bound to the three nitrogen centers are found to be 16, 31, and 32.5 meV. Significant differences between the three centers are discussed.

In Sec. V we show the changes that occur in the nitrogen spectrum at higher temperatures. Additional lines appear, due to the increasing population of a

[1] G. G. Macfarlane, T. P. McLean, J. E. Quarrington, and V. Roberts, Phys. Rev. **108**, 1377 (1957); **111**, 1245 (1958); R. J. Elliott, *ibid.* **108**, 1384 (1957).
[2] J. R. Haynes, Phys. Rev. Letters **4**, 361 (1960).
[3] C. Benoit à la Guillaume and O. Parodi, *Proceedings of the International Conference on Semiconductor Physics, Prague, 1960* (Czechoslovakian Academy of Sciences, Prague, 1961), p. 426.
[4] W. J. Choyke and Lyle Patrick, reference 3, p. 432.
[5] W. G. Spitzer, D. Kleinman, and D. Walsh, Phys. Rev. **113**, 127 (1959).
[6] H. H. Woodbury and G. W. Ludwig, Phys. Rev. **124**, 1083 (1961).
[7] M. A. Lampert, Phys. Rev. Letters **1**, 450 (1958).
[8] Lyle Patrick, following paper [Phys. Rev. **127**, 1878 (1962)].

second valence band, 4.8 meV away, which is split off by spin-orbit interaction. We conclude that the hole is almost completely confined to the carbon sublattice.

In Sec. VI we show the intrinsic lines that appear in the purest samples, and compare these with the nitrogen lines. Both spectra yield the same phonon energies.

The absorption spectrum, shown in Sec. VII, does not yield as accurate band parameters and phonon energies as the exciton recombination radiation. It is most useful in looking for the small-energy phonons. It also permits us to put a lower limit on the exciton binding energy (self-binding), and the valence band separation due to the crystal field.

Our transverse optical (*TO*) branch is consistent with the *TO* value deduced from residual ray data by Spitzer *et al.*,[5] but our longitudinal optical (*LO*) branch is not consistent with the value they calculate for *LO* at $\mathbf{k}=0$ by means of the Lyddane-Sachs-Teller formula.[9] Our *TO* and *LO* phonons occur in groups of three, and allow us to fit some fine structure previously observed in the infra-red lattice combination band spectrum.[10]

Finally, confinement of electrons and holes to Si and C sublattices is considered. Our conclusions are based on the spin-orbit interaction data, and on our interpretation of electron-spin measurements by Woodbury and Ludwig.[6]

II. DESCRIPTION OF SAMPLES

We examined the low-temperature photoluminescence of about 40 crystals of 6*H* SiC, all of which were grown in our laboratories by Hamilton under conditions designed to achieve high purity.[11] Nitrogen, which is difficult to keep out, is the dominant shallow impurity. The nitrogen density varied from about $10^{15}/cm^3$ in the purest samples to about $10^{17}/cm^3$. The crystals also contain perhaps $10^{17}/cm^3$ of deep impurities (mostly Fe-group atoms), but these have no emission lines in the region of the spectrum we are examining here.

All the photoluminescence lines shown in this paper are due to the recombination of excitons, either as free excitons or as excitons bound to un-ionized nitrogen atoms (i.e., in four-particle complexes). In most crystals the spectrum was a mixture of both "intrinsic" and "nitrogen," the proportion of intrinsic being greatest in the crystals with least nitrogen (about $10^{15}/cm^3$). With sufficient nitrogen content the intense nitrogen spectrum obscured the intrinsic part almost completely. Such crystals were used for the 6°K data of Sec. IV, and the higher temperature data of Sec. V. The intrinsic spectrum, shown in Sec. VI, was then obtained by examining the additional lines in the spectrum of those crystals which contained the least nitrogen.

For the absorption measurements, impurities were of little significance. Large samples were cut and polished so as to obtain a long light path (up to 6 mm) perpendicular to the *c* axis, so that polarized light could be used.

The polytype was determined by optical goniometer, and confirmed by the absorption and luminescence spectra. 6*H* is the most common polytype grown in our furnace in high-temperature runs (~2500°C) and many crystals were completely free of any other polytype.

III. EXPERIMENTAL PROCEDURES

The SiC samples were pressed against a copper block through an indium contact. The copper block could be placed in good thermal contact with the helium well of our cryostat, or a small thermal resistance could be interposed to achieve a higher sample temperature, the copper block temperature being measured by a copper-constantan thermocouple. The sample was strongly illuminated by a uv lamp (OSRAM HBO 100 W/1) with a regulated light output. Under illumination the sample temperature is somewhat higher than the copper block temperature. The intensity of several strongly temperature-dependent SiC spectral lines served to provide an internal measurement of the crystal temperature, as discussed in Sec. V. The temperature recorded in this way was always several degrees higher than that recorded by the thermocouple. This result seems plausible, though dependent on a certain interpretation. The temperature we state is an average of the two measurements, which we believe is within 2° of the actual crystal temperature. The lowest temperature we achieved is thus reported as 6°K.

The monochromator polarizes light passing through it to some extent. To correct for this, measurements marked $E\|c$ have been reduced by a factor 2. Because of intensity requirements, most photoluminescence

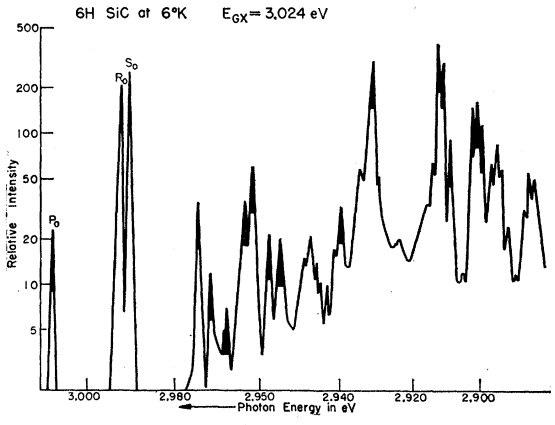

FIG. 1. Photoluminescence spectrum at 6°K due to exciton recombination at nitrogen atoms. The lines marked P_0, R_0, and S_0 are due to recombination without phonon emission at the three inequivalent nitrogen centers. The rest of the spectrum consists of three series of lines displaced from P_0, R_0, and S_0 by phonon emission. The blackened peaks belong to the *P* series, which is considerably stronger than the other two.

[9] R. H. Lyddane, R. G. Sachs, and E. Teller, Phys. Rev. **59**, 673 (1941).
[10] Lyle Patrick and W. J. Choyke, Phys. Rev. **123**, 813 (1961).
[11] D. R. Hamilton, J. Electrochem. Soc. **105**, 735 (1958).

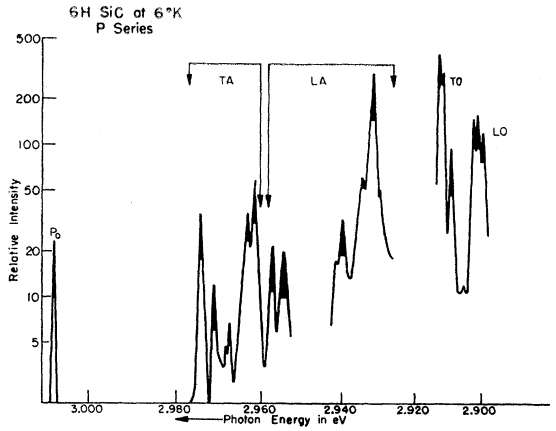

FIG. 2. One of the three series of lines from Fig. 1, the P series, identified by its temperature dependence. The division into TA, LA, TO, and LO is appropriate for an extended zone classification of the phonons.

measurements were made without polarization analysis, and, in these, the measured strengths of strongly polarized lines depend on their polarization direction. No corrections were made in these spectra, but strongly polarized lines are indicated.

IV. NITROGEN SPECTRUM AT 6°K

A. Experimental Results

The letters P, R, and S will be used to refer to the three inequivalent nitrogen centers in $6H$ SiC, or to the three separate spectra which are a consequence of the inequivalent sites.

Figure 1 shows the complete nitrogen spectrum at 6°K. All samples examined had the same intensity ratios for these lines. Occasionally, a sample had extra lines, not shown here, due to unknown impurities. P_0, R_0, and S_0 are the three lines which are due to exciton recombination *without* phonon emission at the three inequivalent un-ionized nitrogen donors. The linewidths are determined by the resolving power of the monochromator. With P_0 is associated a series of lines, the P series, all due to recombination at the P nitrogen center, with emission of one of 17 phonons. Similar series are associated with R_0 and S_0. The displacement of a P line from P_0 measures a phonon energy. Thus, we obtain a spectrum of 17 phonon energies which we shall classify in Sec. IV B. The displacement of P_0 from the exciton energy gap, E_{GX}, measures the binding energy of the exciton to the P nitrogen donor, and is 16 meV. Binding energies to R and S donors are 31 and 32.5 meV. The value of E_{GX} (3.024 eV at 6°K) may be obtained either from the absorption measurements, or, more accurately, from the intrinsic (free exciton) photoluminescence spectrum, provided one phonon energy is known. The usual energy gap, E_G, is greater than E_{GX} by the exciton binding energy (electron-hole binding), which is not accurately known.

In analyzing the complex spectrum of Fig. 1 we are aided by the fact that the exciton binding energy to P donors (16 meV) is considerably less than that to R and S donors. Consequently, an increase in temperature dissociates the P centers more readily than the R and S centers, and so reduces the relative intensity of all P peaks. Thus, the entire P series is easily distinguished by its temperature dependence. A comparison of the three series will be given in Sec. IV D, but for the present we shall consider only the P series. We ignore all R and S peaks and plot only P peaks in Fig. 2; the remaining complexity is now that of the phonon spectrum only.

For $6H$ SiC it has been shown that it is possible to fit ten absorption bands in the infrared as combination bands, using the four phonon energies transverse acoustic (TA)=45 meV, longitudinal acoustic (LA) =67 meV, transverse optic (TO)=95.5 meV, and longitudinal optic (LO)=105.5 meV. These energies are weighted averages over the whole zone, but for relatively flat branches like TO and LO they permit us to identify a group of three of the Fig. 2 peaks as TO, and another group of three as LO. A plausible division of the other peaks into TA and LA is also shown.

More details of these lines are shown in Figs. 3 and 4, with the displacement from P_0, or phonon energy, used as abscissa. Lines that are strongly polarized either parallel (∥) or perpendicular (⊥) to the optic axis are indicated for the acoustical phonons in Fig. 3, and separate drawings are given for the two polarization directions for the optical phonons in Fig. 4.

Further classification of the phonons is suggested by a judicious plotting of their energies against wave vector in an extended **k** space. Experimentally we know the phonon energies but not the wave vectors. In Fig. 5 we have assigned plausible values of k_c to obtain what appears to be a reasonable phonon spectrum. The meaning and the justification of Fig. 5 will be discussed in some detail in the next section. The numerical values of the phonon energies are listed in

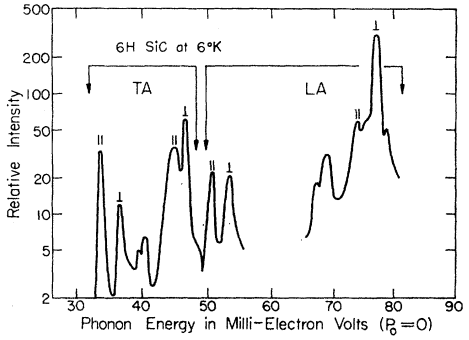

FIG. 3. The acoustic phonon lines of Fig. 2. The abscissa is the displacement of the energy from that of the phonon-free line P_0. Most lines are strongly polarized parallel (∥) or perpendicular (⊥) to the c axis, as indicated in the figure.

Table I, with the same grouping as in Fig. 5. The experimental uncertainty in phonon energies is about 0.5 meV.

B. Phonon Spectrum in Extended k Space

As Jones has stated,[12] an extended **k** space is often convenient when the unit cell contains a large number of atoms. The hexagonal unit cell of 6H SiC contains 6 Si and 6 C atoms. Compared with the wurtzite (2H) unit cell, the a dimension is unchanged, but the c dimension is three times as great.[13] The Brillouin zone of 6H SiC is correspondingly reduced in the c direction,

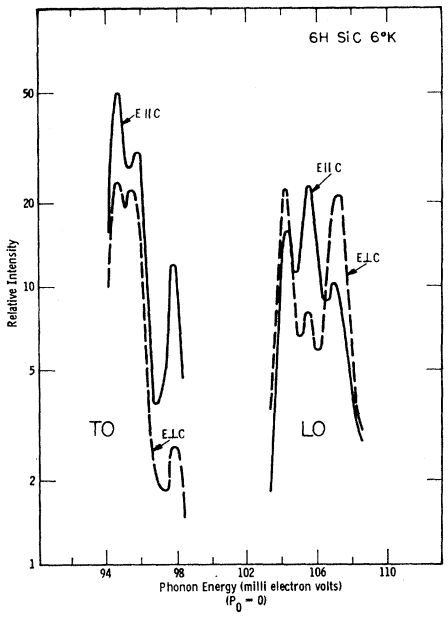

FIG. 4. Optical phonon lines of the P series. The polarization is shown by solid ($E \| c$) and dashed ($E \perp c$) lines.

and it becomes inconveniently small. In Figs. 5 and 6, the abscissa 1, in units of π/c, represents a point on the boundary of the Brillouin zone. The 6 phonon branches of Fig. 5 (including transverse double degeneracy) could be folded into the Brillouin zone to give 36 branches, i.e., three times the number of atoms per unit cell.

TABLE I. Phonon energies in meV.

Phonon branch	$k_c=2\pi/c$	$k_c=4\pi/c$	$k_c=6\pi/c$
TA	33.5 36.3	39.2 40.3	44.0 46.3
LA	50.6 53.5	67.0 69.0	77.0
TO	97.8	95.6	94.7
LO	107.0	105.5	104.2

[12] H. Jones, *The Theory of Brillouin Zones and Electronic States in Crystals* (North-Holland Publishing Company, Amsterdam, 1960), Chap. 5.

[13] A. R. Verma, *Crystal Growth and Dislocations* (Butterworths Scientific Publications, Ltd., London, 1953), Chap. 7.

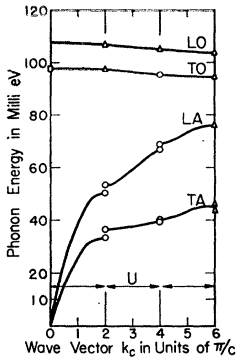

FIG. 5. The 17 measured phonon energies, plotted in a plausible way in an appropriate extended zone, as explained in the text. The abscissa is the c component of the wave vector k_c. ○, from nitrogen spectrum only; △, from both nitrogen and intrinsic spectra; □, determined by Spitzer *et al.* from residual ray data. Possible umklapp processes are denoted by U.

However, for 2H or for 6H SiC, both belonging to space group $P6_3mc$, it is convenient to extend the zone along the c axis as shown in Fig. 6, so that the number of distinct **k** vectors per unit volume of the crystal is equal to the number of Si or C atoms per unit volume. The phonon spectrum drawn in such a zone will have 3 acoustical and 3 optical branches. For 2H SiC the appropriate zone is the Jones zone, and is commonly used. For 6H SiC the appropriate zone is an extended zone cut by planes of energy discontinuity at 2 and 4. If the unit cell length along the c axis is c_2 in 2H and c_6 in 6H SiC, then, since $c_6=3c_2$, a **k** vector $2\pi/c_2$ at the Jones zone boundary in 2H SiC corresponds to the **k** vector $6\pi/c_6$ at the extended zone boundary in 6H SiC. Since the 6H extended zone abscissas 0, 2, 4, and 6 are equivalent in the Brillouin zone scheme, they may be regarded as connected by umklapp (U) processes. Thus, if the conduction-band minima lie at 6, phonons at 0, 2, 4 also satisfy the requirement of

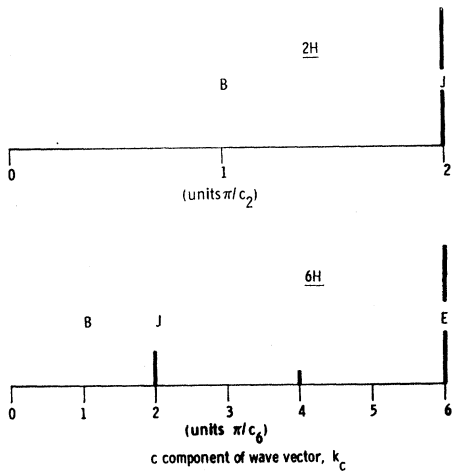

FIG. 6. Schematic comparison of zones in reciprocal space for 2H and 6H SiC. The abscissa, as in Fig. 5, is the c component of the wave vector, k_c. Zone boundaries cut the axis at 1 for the Brillouin zone (B), at 2 for the Jones zone (J), and at 6 for the 6H extended zone (E). Energy discontinuities are indicated schematically by the vertical bars.

crystal momentum conservation. The extended zone has no energy discontinuities at odd values of π/c because, in both $2H$ and $6H$ SiC, the space group operation 6_3 ensures the vanishing of Fourier coefficients of the potential of the type $V_{00\cdot l}$ where l is odd.

It is instructive to think of the $6H$ extended zone as being derived from the $2H$ Jones zone by the addition of a potential associated with a lattice superstructure. One result of a superstructure potential, as pointed out by Slater[14] for alloy or magnetic ordering, is to introduce new energy discontinuities in $\mathbf{k}$ space. For the purpose of evaluating Fourier coefficients of the type $V_{00\cdot l}$, the close-packed planes of the $2H$ structure may be considered to be identical, but in $6H$ SiC the planes are inequivalent in the same way that P, R, and S sites are inequivalent. The largest part of the superperiodicity in $6H$ SiC is probably that which distinguishes every third plane of Si or C atoms perpendicular to the c axis, as P sites are apparently quite different from R and S sites. The $V_{00\cdot 2}$ Fourier coefficient has this periodicity $(c/2)$ and is associated with the energy discontinuity at 2. The relative strengths of energy discontinuities at 2, 4, and 6 are suggested schematically in Fig. 6 by the heights of the vertical bars.

Electron, hole, and phonon states are, from this point of view, mixed by the superlattice potential. However, since $V_{00\cdot 1}$ vanishes, there is no *first*-order mixing of states separated by only 2 units of π/c, such as those at 6 and 4. The mixing of states at 6 and 2 is due to $V_{00\cdot 2}$ and should be relatively strong.

The following plausible assignment of c components of $\mathbf{k}$ vectors to the 17 observed phonon energies can now be made. The groups of three TO and three LO phonons are plotted at 2, 4, and 6 in Fig. 5. The six TA phonons can be assigned to 2, 4, and 6 in pairs. The same can be done for five LA phonons, placing only one at 6. (The 73.8-meV peak appears to be a two-phonon peak, namely, 33.5 plus 40.3.) We believe that the double degeneracy of the transverse branches is not resolved except for TA at 6. The other splittings in the acoustic branches are attributed to the energy discontinuities at 2 and 4. Note that, at 2, the TA splitting is comparable with that of LA, in which no double degeneracy exists. Also the splitting at 2 is greater than that at 4, as expected if $V_{00\cdot 2}$ is indeed the largest component of the superlattice potential. The splittings in the flat optical branches are expected to be quite small. We think we have just barely resolved the two LO peaks at 2. Thus, the fact that we observe 17 phonons and not 30 (omitting the 6 at $\mathbf{k}=0$) is thought to be due primarily to our failure to resolve a number of multiple peaks. The absence of phonons at $\mathbf{k}=0$ is discussed below.

All points in Fig. 5 represent phonon energies found in the nitrogen spectrum, except the square point at $\mathbf{k}=0$ on the TO branch. That point is plotted at the energy found by Spitzer *et al.*[5] in fitting residual ray data for light propagating along the optic axis, and it appears to be consistent with our assignment of phonon energies. Several phonons, marked by triangles, have also been found in the intrinsic spectrum (Sec. VI), with energies indistinguishable from those of the nitrogen spectrum. We believe this indicates that the presence of the nitrogen donor has little effect on the phonon energies found here, so that they may all be considered to be lattice phonon energies.

If the conduction-band minima are at 6, the acoustic phonons emitted in exciton recombination should be principally those at 6, as they appear to be, but also those at 0, 2, and 4 to the extent that those states are mixed in by the superstructure potential. Apparently this is a partial explanation of the intensities of the phonon lines plotted at 2 and 4, and also of the absence of phonons at 0.

C. Conduction Band Minima

We shall assume that the valence band maxima are at $\mathbf{k}=0$. The valence band splittings are discussed in Sec. V B. The positions of the conduction band minima are then partly determined by the phonon assignments of Fig. 5, which require k_c for the minima to be 0, 2, 4, or 6 (in units of π/c). The much greater intensity of the peaks plotted at 6 in the acoustic branches suggests $k_c=6\pi/c$. The component of $\mathbf{k}$ perpendicular to the c axis is undetermined, but the observation of two TA branches, implied by our phonon assignment at 6, requires the conduction band minima to be *off* the hexagonal axis, for the two TA branches are degenerate in that direction. Thus, a many-valley model is appropriate, perhaps with six valleys. It also follows that the wave vectors of the phonons plotted at 2, 4, and 6 in Fig. 5 are not collinear. Our plot shows only the c components, k_c, of the wave vectors.

If we had independent measurements of the phonon spectrum, such as the neutron scattering measurements for Ge[15] and Si,[16] we could use our measured phonon values to locate the conduction band minima. The TA values might be particularly useful if the TA branches were like those of Ge, strongly anisotropic,[15] with the separation of the two TA branches also dependent on direction.[17] One might be tempted to use a scaling procedure to make a comparison with Ge and Si, even though $6H$ SiC is ionic and uniaxial. However, there is good evidence that even the diamond phonon spectrum[18] is not related to the Ge and Si spectra by a scaling factor, but is qualitatively very different, especially in the TA branches. Hence, a comparison of SiC with Ge and Si is probably not useful.

[14] J. C. Slater, Phys. Rev. **82**, 538 (1951).

[15] B. N. Brockhouse and P. K. Iyengar, Phys. Rev. **111**, 747 (1958).

[16] B. N. Brockhouse, Phys. Rev. Letters **2**, 256 (1959).

[17] J. C. Phillips, Phys. Rev. **113**, 147 (1959).

[18] J. R. Hardy and S. D. Smith, Phil. Mag. **6**, 1163 (1961).

We conclude that the conduction band minima probably lie in a plane perpendicular to the c axis, and cutting the c axis at $k_c=6\pi/c$. They may lie in the intersections of this plane by the vertical reflection planes, which contain vectors corresponding to the $\langle 111\rangle$ and $\langle 100\rangle$ vectors of the Ge or Si reciprocal lattice.

D. Relative Intensities of P, R, and S Series

The electron-spin-resonance data of Woodbury and Ludwig[6] indicate that nitrogen in 6H SiC is equally distributed over the three available sites. Thus, a comparison of the three series of lines sheds light on certain properties of the three inequivalent nitrogen donors. The identification of P, R, and S with specific sites is still uncertain.[8] When a positive identification has been made, 6H SiC will serve to test theoretical calculations of the effect of the nitrogen donor environment on the properties discussed below.

The total recombination rate at one of the three sites is found by integrating over a series of lines. We find experimentally that the recombination rate at the P site is four or five times larger than the rate at the R or S sites, R and S rates being very similar. The recombination rate depends on capture, dissociation, and recombination probabilities. Dissociation is important at higher temperatures (Sec. V), but is negligible at 6°K; hence, no quasi-equilibrium is established in the population densities of the four-particle complexes. The recombination rate would be important in determining the intensities only if the complexes were approaching saturation, which they are not, as the photoluminescence intensity is proportional to the uv excitation intensity in our experiments. Hence, the greater P-site recombination rate is an indication of a larger P-site exciton capture cross section. This is consistent with the expectation that the van der Waals attraction between the two hydrogen-like entities of exciton and neutral donor should be greater for the donor with the larger radius, i.e., for the more loosely bound P-site donor.

Exciton recombination in 6H SiC requires an indirect transition, hence recombination without phonon absorption or emission is forbidden for free excitons. The localization of the exciton by binding to a donor makes the P_0, R_0, and S_0 lines possible. At 6°K the R_0 and S_0 lines are considerably stronger than P_0, even though the R and S series are weaker than the P series. This is consistent with the stronger binding, hence great localization, of the exciton at the R and S sites.

The relative intensities and polarizations of lines other than the zero-phonon lines appears to be approximately the same within each of the three series. These intensities and polarizations are determined by electron-phonon interaction strengths, the extent of the state mixing by the crystal potential, and selection rules. An analysis of symmetry types, like that of Lax and Hopfield[19] for Ge and Si would help to explain the polarization, and might serve to locate the conduction-band minima.

[19] M. Lax and J. J. Hopfield, Phys. Rev. 124, 115 (1961).

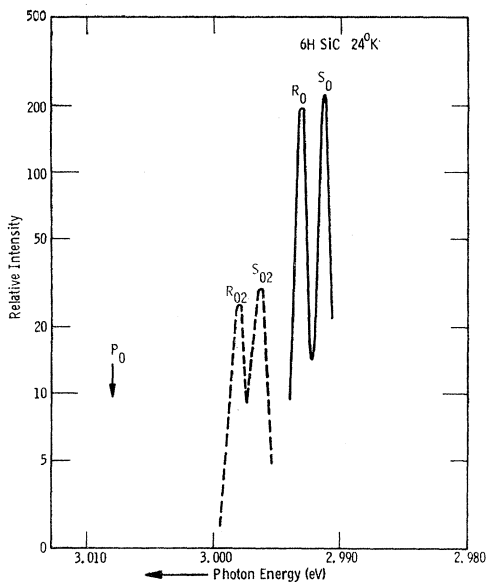

FIG. 7. Nitrogen spectrum at 24°K. The position of the line P_0 at 6°K is indicated by an arrow. Lines R_{02} and S_{02}, absent at 6°K, are shown as dashed lines.

V. NITROGEN SPECTRUM ABOVE 6°K

A. Experimental Results

When the temperature is increased two important changes are observed in the nitrogen spectrum. (1) The relative intensity of the P series rapidly decreases. (2) A new spectrum appears which is a duplicate of the old spectrum but displaced 4.8±0.3 meV toward higher energies; and the new spectrum grows with temperature at a rate given by a Boltzmann factor. Figure 7 illustrates these two points by showing the high-energy end of the spectrum at 24°K. The letter P_0 in Fig. 7 indicates the energy of the now missing P_0 line. The lines marked R_{02} and S_{02} are the lines of the new spectrum which are displaced 4.8 meV from R_0 and S_0, respectively. They are polarized primarily $E\perp c$, like R_0 and S_0.

The duplicate spectrum can be resolved only for the strongest lines, but P, R, and S lines have been observed, and the displacement is 4.8 meV in all three series. Lines in the duplicate spectrum appear to have the same polarization as the corresponding undisplaced lines, but their low intensities allow possible errors of about 20% in polarization ratios. Each peak has an intensity related to that of the undisplaced peak by $\exp(-\Delta E/kT)$, where ΔE is 4.8 meV. In the following section we relate ΔE to the spin-orbit splitting of the valence bands.

The decrease in the P series intensity should be observed when dissociation becomes significant for the weakly bound P complex. At 15°K the ratio of P

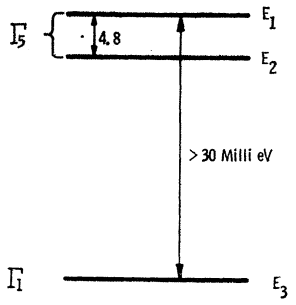

FIG. 8. Observed splittings of the three valence bands. The small spin-orbit interaction splits E_1 and E_2, and a much larger crystal field interaction splits off E_3.

intensities to R and S intensities is about half its 6°K value, which means that dissociation and recombination are equally probable at P sites. Hence, we equate the dissociation frequency $\nu_1 \exp(-E/kT)$ and the recombination frequency ν_2, where E is 16 meV, the P-site binding energy. We find $\nu_1 \cong 10^5 \nu_2$. If we take ν_1 to be a lattice frequency, say 10^{13} sec^{-1}, we find that ν_2 is 10^8, a plausible frequency for atomic transitions.

B. Valence Band Structure

The valence band structure of uniaxial 6H SiC is expected to be similar to those of ZnO and CdS, which have been analyzed by Hopfield.[20] Both spin-orbit and crystal field interactions have to be considered, and the valence band splittings are determined by a combination of the two interactions. In 6H SiC the crystal field energy is thought to be considerably greater than the spin-orbit energy, so that the spin-orbit mixing of the second and third valence bands should be small. Hence, the polarization properties may be approximated by considering the single group representations of the valence bands as indicated in Fig. 8.

Figure 8 is based on the observation of the two sets of exciton recombination lines separated by 4.8 meV and having the same polarization; and on a lower limit of 30 meV for E_1-E_3 obtained from the absorption spectrum (Sec. VII). Our photoluminescence measurements involve a hole bound in a four-particle complex, but we assume that the measured 4.8 meV is nevertheless a good approximation to the valence band separation E_1-E_2. We have seen no evidence of the third valence band either in the luminescence or in the absorption measurements, so E_1-E_3 could be *much* greater than 30 meV, in which case the valence band separation 4.8 meV could also be taken as the spin-orbit energy. From the 30 meV lower limit on E_1-E_3 we can obtain an upper limit of 8 meV on the spin-orbit energy by using the formulas in Hopfield's paper.[20]

The spin-orbit energy in Si is 44 meV, as reported by Zwerdling *et al.*[21] The spin-orbit energy in diamond is not known, but a rough estimate of 4 meV can be made by using the values obtained from atomic spectra. In SiC the spin-orbit energy is determined by the Si and C interactions, and the fractional time spent by a valence electron on the Si and C sublattices.[22] The considerable difference in atomic sizes of Si and C result in a quite large effective charge (~0.94) for the Si and C atoms,[5] with the excess electron density on the C atom. Hence, we expect a SiC spin-orbit energy considerably closer to the C value than to the Si value. Thus, the range of spin-orbit energies determined by our measurements (4.8 to 8 meV) is plausible. Using the upper limit of 8 meV, we conclude that the hole spends no more than 10% of the time on the Si sublattice.

VI. INTRINSIC PHOTOLUMINESCENCE SPECTRUM

The intrinsic spectrum, due to recombination of free excitons, was observed against a background of the nitrogen spectrum. Only a few lines of the intrinsic spectrum are well separated from nitrogen lines. Figure 9 shows two such lines in the high-energy portion of the spectrum at 6°K. They are identified as I 44 and I 46.3, the numbers being the phonon energies in meV. In Fig. 9 one might expect to observe intrinsic lines involving all the TA phonons. The pair of lines shown is plotted at 6 in Fig. 5. The intrinsic lines corresponding to the nitrogen lines plotted at 2 and 4 in Fig. 5 are, respectively, hidden by S_0, and hidden by the background. All intrinsic lines observed are indicated by triangles in Fig. 5.

Because of interference by the nitrogen spectrum, we do not have accurate values of the relative intensities or polarizations in the intrinsic spectrum. In these respects we can only say that the intrinsic and nitrogen spectra are different, but not *very* different. For example, in both spectra the TA and LA peaks plotted at

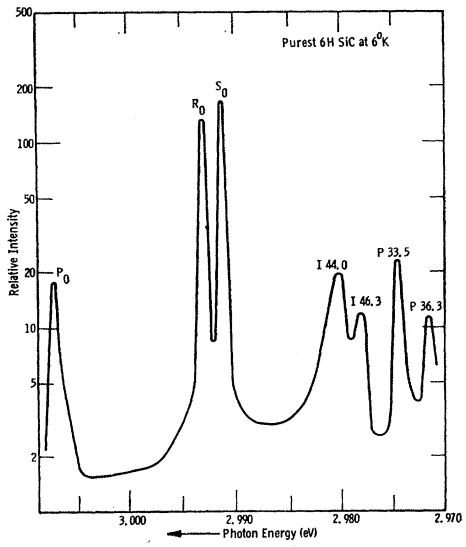

FIG. 9. Purest sample at 6°K, showing two additional intrinsic lines (I 44.0 and I 46.3) due to the recombination of free excitons.

[20] J. J. Hopfield, J. Phys. Chem. Solids **15**, 97 (1960).
[21] S. Zwerdling, K. J. Button, B. Lax, and L. M. Roth, Phys. Rev. Letters 4, 173 (1960).
[22] R. Braunstein, J. Phys. Chem. Solids 8, 280 (1959).

6 in Fig. 5 are very much stronger than those at 2 and 4, and the direction of polarization is the same, although the degree of polarization is somewhat different. We will not give any detailed description of the differences, as we do not use this information in our interpretation.

The phonon energies derived from the intrinsic spectrum are less accurate than those derived from the nitrogen spectrum, but in the lines we have observed we find no differences (within experimental error of about 1 meV). We conclude that the presence of the nitrogen atom has little effect on the observed phonon energy.

The shape expected for intrinsic lines may be derived, by a consideration of detailed balance, from the energy dependence of the corresponding part of the absorption spectrum.[23] To a very good approximation, the shape should be $(\Delta E)^{1/2}\exp(-\Delta E/kT)$, where $\Delta E=E-E_{GX}+k\theta$, E is the photon energy, E_{GX} is the exciton energy gap, and $k\theta$ is the phonon energy. The line I 44 of Fig. 9 can be fitted by this expression fairly well, but only with a value of T which is approximately twice the measured temperature.

VII. ABSORPTION SPECTRUM

Following the early work on the absorption edge of Ge and Si by Macfarlane and Roberts,[24] we identified the absorption edge transitions in 6H SiC as indirect,[25] but used only a single phonon in fitting the data. Later, following better work on Ge and Si,[1] we measured the 6H SiC edge more accurately, and made a better fit to the data by using three phonons,[4] and by recognizing *exciton* absorption. It is now apparent, from the recombination radiation, that very accurate fitting of the edge would require at least 17 phonons. At 77°K, where phonon absorption processes are still negligible in 6H SiC, the extreme edge involves the emission of only one phonon (the smallest), but within 0.1 eV of the edge all phonons are active, and it is impossible to decipher the various contributions with any accuracy.

Thus, the absorption spectrum is, in most respects, much less useful than is the line spectrum of the recombination radiation. We shall, therefore, point out only the main features of the absorption spectrum, with special attention to the initial portion in which only a few of the phonons are active.

A. Experimental Results

Figure 10 shows the two absorption edges of 6H SiC over an energy range of 0.1 eV, obtained by measuring the relative transmission of polarized light through the sample, as a function of the photon energy. Most measurements were made at 77°K. Unlike the photoluminescence, there is no significant difference between

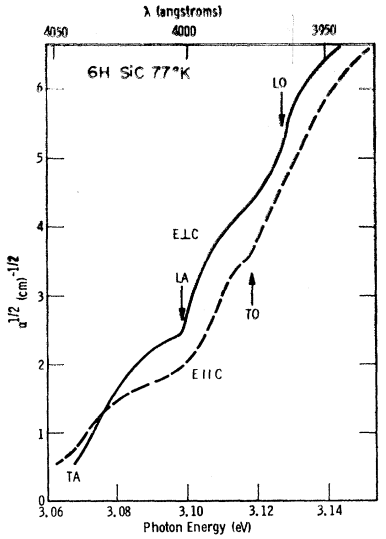

FIG. 10. Absorption edges of 6H SiC in polarized light at 77°K. In this region excitons are formed with the emission of one of 17 phonons. The shapes of the two edges are largely determined by a smaller number of phonons, as discussed in the text.

6 and 77°K measurements, except for an energy shift of about 1 meV.

We have plotted the square root of the absorption coefficient ($\alpha^{1/2}$) against photon energy, as is usually done for indirect transitions. For 6H SiC, such a plot is linear for photon energies greater than 3.2 eV, as expected for transitions resulting in electron-hole pairs.[4] In the region shown in Fig. 10, however, excitons are formed with the emission of one of 17 or more phonons. The transitions are from two, and possibly three valence bands. Because the transitions from the two top valence bands have the same polarization and are separated by only 4.8 meV, the absorption edges are merely broadened for the resolution employed in these measurements.

We shall use our knowledge of the phonon spectrum, obtained in the photoluminescence experiments, to point out the main features of Fig. 10. With increasing photon energy, changes in curvature are observed as the dominant phonons become active. The phonons making the largest contributions are 44.0 meV ($E\|c$) and 46.3 ($E\perp c$) at TA, 77.0 ($E\perp c$) at LA, a group of three TO phonons (primarily $E\|c$) at TO, and a group of three LO phonons at LO. The intensities and polarizations of the various contributions to the absorption depend not only on selection rules for the optical transitions, but also on selection rules for the electron-phonon and hole-phonon scattering. The necessary symmetry analysis has not yet been done for 6H SiC.

Up to 3.10 eV the absorption is determined largely by a single phonon in each polarization direction. To examine this region in more detail we used a large crystal (light path ~6 mm) and in Fig. 11 we have plotted the relative transmission of this crystal (on an

[23] W. van Roosbroeck and W. Shockley, Phys. Rev. **94**, 1558 (1954).
[24] G. G. Macfarlane and V. Roberts, Phys. Rev. **97**, 1714 (1955); **98**, 1865 (1955).
[25] W. J. Choyke and Lyle Patrick, Phys. Rev. **105**, 1721 (1957).

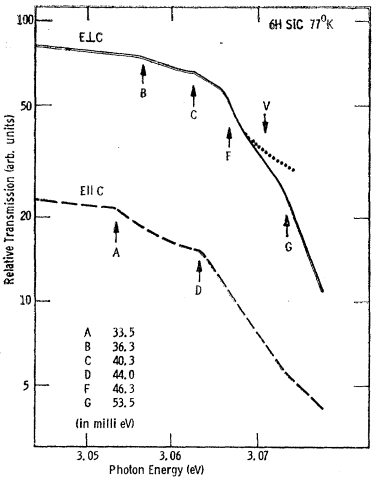

FIG. 11. Relative transmission of polarized light through a thick (6 mm) crystal at 77°K. The separation of the two curves is arbitrary. The letters refer to breaks in the curves at which emission processes become possible for the listed phonons. The dotted curve is a theoretical curve fitted at F. The departure from it (near V) of the experimental curve is attributed to absorption from the second valence band (E_2 of Fig. 8).

arbitrary scale). We again use our knowledge of the phonon spectrum to identify phonons associated with the various changes in curvature, as indicated in the figure by letters. Four of these six phonons were not observed in the intrinsic photoluminescence spectrum because they were hidden by the nitrogen spectrum. However, the breaks in Fig. 11 are not adequate to make possible a quantitative comparison of phonon energies with those obtained from the nitrogen spectrum. The values listed in Fig. 11 are therefore those obtained from the nitrogen spectrum.

In the $E\perp c$ curve, the sharpest break is due to the 46.3-meV phonon, and we have fitted that portion, beginning at F, with the theoretical curve $\alpha=A(\Delta E)^{1/2}$, where ΔE is the energy measured from F, and A is a constant. The experimental curve deviates from the theoretical curve near V, where absorption from the second valence band is expected to begin. A more definite break would have been observed if the edge were as sharp as that at F. Thus, it appears that the absorption edge due to transitions from the second valence band is broadened. Macfarlane *et al.* have related such broadening in Si to scattering.[1] This is a possible explanation of the extra broadening here, since hole scattering from the second to the first valence band is possible.

There is likely to be a strong absorption due to the third valence band, involving either the 44.0- or the 46.3-meV phonon. This absorption probably could be observed if it occurred below 3.10 eV. Thus, from the fact that we do not observe it, we deduce 30 meV as a lower limit for E_1-E_3 in Fig. 8. This conclusion is reinforced by the observation (Sec. V B) of similar polarization of the spectra due to the two top valence bands, which indicates that spin-orbit mixing of the second and third valence bands is small, hence, that the separation is large.

Similarly, no absorption was observed below 3.10 eV which could be attributed to transitions resulting in electron-hole pairs. Hence, 30 meV may also be taken as a lower limit for the exciton binding energy.

B. Temperature Dependence of E_{GX}

The sharpest break in the absorption is at 3.10 eV in the $E\perp c$ curve (at LA in Fig. 10). This break can be observed up to 200°K, beyond which it becomes too indistinct to measure accurately. We have used the temperature dependence of this break to plot, in Fig. 12, the temperature dependence of the exciton energy gap E_{GX}. The usual energy gap E_G is larger than E_{GX} by the still unknown exciton binding energy.

At higher temperatures no sharp breaks in the absorption can be seen. An approximate value of the temperature dependence of the energy gap above room temperature is -3.3×10^{-4} eV/deg, as obtained in reference 26 from a one-phonon fit of the absorption.

VIII. DISCUSSION OF PHONON SPECTRUM

Evidence of a complex phonon spectrum in 6H SiC was previously seen in our infrared combination band measurements,[10] and possibly also in Raman scattering measurements by Mathieu and Poulet.[26] The latter apparently did not determine which hexagonal polytype they used, but they reported six lattice frequencies, of which two are identical with the 94.7- and 97.8-meV TO phonons reported here.

The combination band measurements showed structure in two bands identified as the two-phonon emission bands $2TO$ and $TO+LO$. This structure is related to singular points in the density of states curves for the TO and LO phonon branches, and one would expect to find singular points associated with the energy discontinuities at 2, 4, and 6 in Fig. 5. The crystal momentum selection rule for two-phonon processes is that the two momenta should be equal and opposite. Thus, neglecting mixing of states, there should be bands corresponding to the densities at 2, 4, and 6. Figure 13 is from our earlier paper,[10] and we have added the arrows indicating the two-phonon processes with the TO and LO phonon energies of Table I. The latter refer to particular directions in $\mathbf{k}$ space and cannot be expected to fit the two-phonon bands exactly, but we believe the fit is good enough to make our explanation of the structure plausible.

Our TO phonon energies are compatible with the $\mathbf{k}=0$ residual ray value of 98.4 meV reported by Spitzer *et al.*[5] However, our LO phonon energies appear to be incompatible with their calculated value of 120 meV for the LO phonon at $\mathbf{k}=0$, using the Lyddane-

[26] J. P. Mathieu and H. Poulet, Compt. rend. **244**, 2794 (1957).

Sachs-Teller[9] formula. Mathieu and Poulet[26] reported evidence in the Raman scattering for two phonon energies in the neighborhood of 120 meV, but we have observed nothing in this region, either in the photoluminescence, or in the infrared combination band spectra. The $\mathbf{k}=0$ phonons do not contribute to our measurements, however, and the possibility remains that the *LO* phonon branch may rise sharply toward a value of 120 meV at $\mathbf{k}=0$.

IX. CONFINEMENT OF ELECTRONS AND HOLES TO DIFFERENT SUBLATTICES

The measurement of spin-orbit interaction indicated that the hole is largely confined to the carbon sublattice. Electron spin measurements by Woodbury and Ludwig,[6] as we interpret them below, suggest that the electron is largely confined to the silicon sublattice.

To explain the small observed amplitude at the N nucleus,[27] Woodbury and Ludwig suggested that the electron wave function is spread out in a large orbit. Noting the comparison with P in Si, we think their explanation is improbable, in view of the much larger ionization energies for N in SiC (using the estimate $E_i=10E_D$).[8] Instead, it seems more likely that the electron density at the N nucleus is small because N substitutes for C, and the electron density on the C sublattice is small. A pertinent experiment would be a measurement of the electron spin resonance of P, substituting for Si in SiC.

A similar confinement of holes and electrons to separate sublattices[28] has been noted in Bi_2Te_3. One consequence, for SiC, is that it may be desirable, in growing high-mobility crystals, to reduce impurity scattering as suggested in reference 28, i.e., by doping with donors which substitute for C, as N does, or with acceptors which substitute for Si, as Al does.

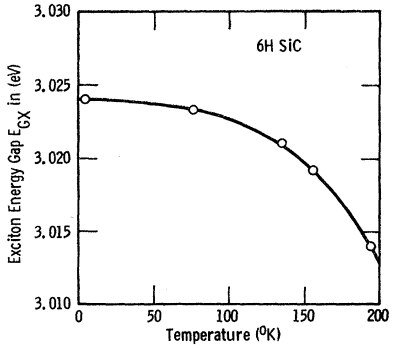

FIG. 12. Temperature dependence of the exciton energy gap E_{GX}, obtained by measuring the temperature dependence of a sharp edge in the absorption spectrum.

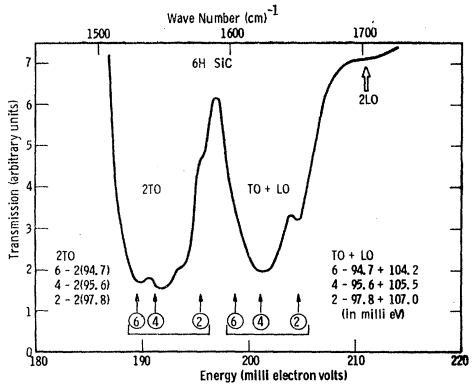

FIG. 13. The previously reported structured absorption in certain two-phonon lattice bands, together with arrows denoting two-phonon energies derived from the present work. The numbers 2, 4, and 6 in the arrows and before the phonon energies indicate the k_c values of the phonons as plotted in Fig. 5.

[27] The fact that one value of E_D is quite different from the other two suggests that the electron wave function of one N donor is quite different in the neighborhood of the N atom. Nevertheless, Woodbury and Ludwig find that the difference in the hyperfine interaction at the unique site is only 1%; hence; the wave function difference is scarcely felt within the N atom.

[28] A. F. Joffe and L. S. Stil'bans, *Reports on Progress in Physics* (The Physical Society, London, 1959), Vol. XXII, p. 167.